

ITER ECRF UPPER LAUNCHER OPTIMISATION STUDIES

G.Ramponi, D.Farina, S.Nowak

Istituto di Fisica del Plasma, EURATOM-ENEA-CNR Association

Via Cozzi 53, 20125, Milano (Italy)

e-mail: ramponi@ifp.cnr.it

The quasi-optical ECWGB code is used to predict the design requirements and performances of the ITER-ECRF Upper Launcher, that has as its main goal the stabilization of (3,2) and (2,1) neoclassical tearing modes. Detailed calculations are presented here for various ITER-FEAT relevant plasma scenarios. The required steering range and the behavior of figures of merit for NTMs stabilization are shown for both the upper and lower row of mirrors, pointing out that larger efficiencies are obtained by launching from the lower row. The effect of the local beam size on the width of the driven current profile is underlined.

1. Introduction

The main task of the ITER Upper Launcher is the stabilization of (3,2) and (2,1) neoclassical tearing modes (NTM's) by localized electron cyclotron current drive. This task requires the capability to drive a current well localized at the relevant q rational surfaces, with maximum driven current I_{EC} and minimum current profile width 'd'. The capability of localize the current at the relevant surfaces for a variety of plasmas requires that the EC beams, injected with an 'optimum' toroidal angle (compromise between large I_{EC} and minimum 'd') are steered in the poloidal angle. In present study we adopt the ratios I_{EC}/d or I_{EC}/d^2 as figures of merit for NTMs stabilization by means of modulated or not modulated EC power respectively [1].

Calculations made with the 'quasi optical' ECWGB code [2] are presented here, for various ITER scenarios relevant for NTMs and for Upper Launcher specifications compatible with present conceptual design. The goal of the work has been to evaluate the performance of the present design of the Upper Launcher in close contact with the design team, in order to optimize the system. The performance specification includes that of the required poloidal steering range that may have consequences on the final design of the last mirrors.

The paper is structured as follows. In Sec.2 the physical model of ECWGB code is summarized and the toroidal and poloidal angles used in the calculation are defined. In Sect. 3 the main parameters of the considered ITER equilibria are listed and in Sect.4 the beam geometry is specified. In Sect.5 the results for the figures of merit as a function of the toroidal injection angle are shown for both upper and lower row, as well as the combined steering range. Moreover the performances of the present launcher design are evaluated in terms of the ratio of the peak driven current density and the local bootstrap current. In Sect.6 the ef-

fect of the local beam size on the width of the driven current profile is pointed out.

2. Physical Model And Launching Angles

ECWGB solves the quasi-optical propagation equations of a gaussian beam in a general toroidal magnetic equilibrium [2]. On each ray of the beam the weakly relativistic EC power absorption is computed as well as the relativistic EC current drive. In the cylindrical reference system (ρ, R, Z) the ITER launching angles (θ, ϕ) are defined as $\theta = \tan^{-1}(N_z/N_R)$, $\phi = \sin^{-1} N_\rho$ so that the parallel component of the refractive index reads

$$n_{//} = \sin \theta b_\rho \cos \phi \cos \theta b_R \cos \theta \sin \theta b_z \quad (1)$$

It should be noticed that for ITER equilibria $n_{//}$ has to be negative in order to drive a co-current and that the angles (θ, ϕ) assume different values at the mirror and at the launching virtual points, which are located at different ρ .

3. ITER Scenarios and Equilibria

We have considered three ITER scenarios and five equilibria. For the reference scenario 2 (inductive, $Q=10$, 15MA, $T_{e0}=24.8$ keV, $n_{e0}=1.02 \times 10^{20} \text{ m}^{-3}$) three equilibria with different values of the internal inductance l_i have been taken into account leading to a variation of the location of resonant surfaces (the case $l_i=0.76$ is the so-called ‘Gribov’ case [3]). In addition scenario 3 (hybrid operation at reduced $I_p=13.8$ MA) and scenario 5 (low q operation at increased $I_p=17$ MA) have been studied. The equilibria are given through EQDSK files [4]. The plasma profiles are the same as for scenario 2 but rescaled in case of scenario 5 and 3 in order to keep the same ratio n/n_G and to be consistent with the variation of the poloidal ψ . The main plasma parameters are listed in Table I.

Table I

Case	I MA	ψ_p	$n_{e0}/10^{20}$ m^{-3}	T_{e0} keV	R_{axis} m	Z_{axis} m	B_{axis} T	$\psi_{3/2}$	$\psi_{2/1}$
<i>Sob2_0.7</i>	15	0.65	1.02	24.8	6.41	0.57	5.25	0.495	0.735
<i>Gribov</i>	15	0.65	1.02	24.8	6.41	0.68	5.32	0.605	0.770
<i>Sob2_1</i>	15	0.65	1.02	24.8	6.41	0.55	5.33	0.730	0.825
<i>Sob3_0.7</i>	13.5	0.80	0.92	27.5	6.42	0.58	5.18	0.380	0.670
<i>Sob5_0.7</i>	17	0.70	1.15	30.2	6.45	0.65	5.24	0.635	0.805

Note that a large range of the normalized flux function ψ for the relevant surfaces has been considered and that the case Sob 3 has a magnetic field lower than other cases. The geometry of the relevant surfaces in the upper region of the (R, Z) plane, where ECW absorption occurs, mostly determines the required steering range and is shown in ref. [1].

4. Beam geometry and parameters

The reference conceptual design presently foresees to install three launcher modules, each comprising of 8 beams, with a total power capability in the plasma $P=20$ MW at $f=170$ GHz which can be switched between the upper and equatorial launchers. In each module two rows (Upper & Lower row) of four ‘last fixed mirrors’ reflect into the plasma toroidally directed beams coming from the output of transmission lines remotely steered. Here one mirror in the upper and one in the lower row are considered, located at $(R=6.49\text{m}, Z=4.50\text{m})$ and $(R=6.95\text{m}, Z=4.36\text{m})$ respectively. The two focused beams are characterized by having their waist $w_0=1.82\text{cm}$ at a distance $\Delta=-8.6\text{cm}$ from the upper mirror and $w_0=1.68\text{cm}$ at a distance $\Delta=-2.7\text{cm}$ from the lower mirror (negative Δ means behind the mirror)[5].

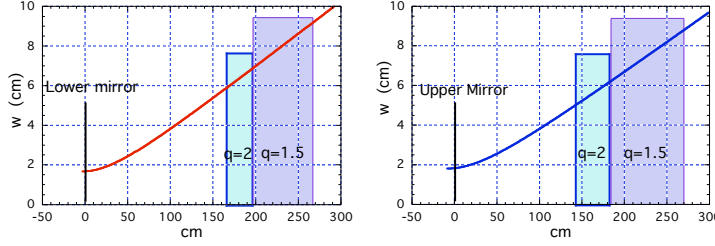


Fig.1: Evolution (in vacuum) of the beam radius at e-2 of peak power for Lower (left) and Upper (right) beams.

5. Results for Upper and Lower Rows

The behaviour of the figures of merit I_{EC}/d and I_{EC}/d^2 at $q=2$ as a function of the toroidal angle Δ (at the mirror mid-point) is shown in Figs.2 and 3 respectively, for $P_{EC}=1\text{MW}$, all scenarios and for the lower and upper rows. In the figures the full width d is computed as the distance between the two Δ locations (here Δ is the normalized poloidal radius) where the current density profile is $1/e$ of its peak value.

Note that for I_{EC}/d the values of ‘optimum’ Δ (the value where figures of merit have their maximum) are in a range from $\sim 18^\circ$ (scenario3) to $\sim 22^\circ$ (scenario5) for lower row, in a range from $\sim 16^\circ$ (scenario3) to $\sim 20^\circ$ (scenario5) for upper row. The values of optimum Δ for I_{EC}/d^2 are still lower because of the larger weight of d , which is smaller at lower values of $N_{//}$. It may be also noticed that the stabilization efficiencies obtained launching from upper row are reduced respect to that from lower row, mainly because of a larger profile width. This occurs despite the size in vacuum of the lower beam at the resonant surfaces is larger than that of the upper beam (see Fig.1), and is due to the different geometry of the trajectories in the absorption region with respect to Δ . A similar behavior is found for $q=3/2$.

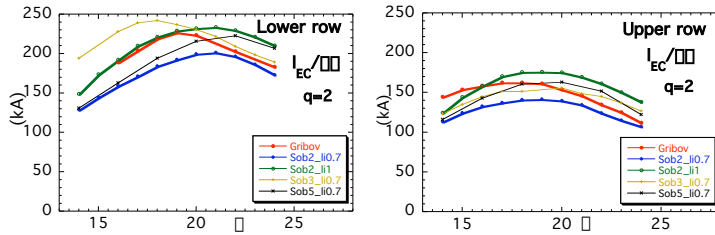


Fig.2: Figures of merit for NTMs stabilization by means of modulated ECCD at $q=2$. a is the adimensional poloidal full width.

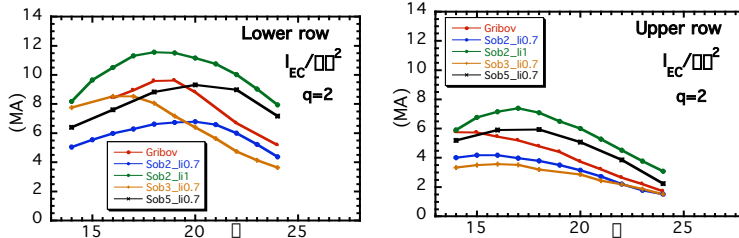


Fig.3: Figures of merit for NTMs stabilization by means of non modulated ECCD at $q=2$.

In Fig.4 the relation between poloidal and toroidal angles (at the last mirrors) to localize the driven current at the relevant surfaces is shown for both lower and upper rows. It turns out that the steering range required to reach both surfaces should be at least $\pm 10.5^\circ$ for lower row at $\alpha=20^\circ$, and $\pm 8^\circ$ for upper row at $\alpha=18^\circ$.

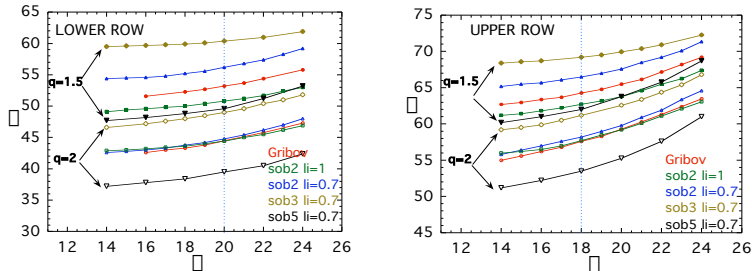


Fig.4: Poloidal vs. toroidal angles for lower (right) and upper (left) row

For mechanical constraint, the remote steering launcher appears to have a trade off between the beam focusing and the steering range. The beam parameters we used in present calculations are consistent with a vertical steering of $\pm 7.5^\circ$ for upper row and $\pm 8^\circ$ for upper row at the front mirror. The reduced steering range required for launchers dedicated to reach only $q=2$ or $q=3/2$ surfaces would improve the focusing of the beams, leading to higher stabilization efficiencies.

Taking into account that for ITER parameters the EC current is linearly related with the injected power [6], the ratios of the peak EC current density corre-

sponding to $P_{EC}=20$ MW and the local bootstrap current density are easily evaluated for dedicated launchers (with present beams) and are shown in Table II for $q=3/2$ and in Table III for $q=2$.

Table II

Case sob2	\square	\square_m	\square_m	J_{bs} (kA/m ²)	J_{peak} (kA/m ²)	J_{peak}/J_{bs}
<i>li=0.7 (10MW U)</i>	.495	18	66.5		35.4	
<i>li=0.7 (10MW L)</i>	.495	20	56.2		66.9	
<i>li=0.7 (U+L)</i>	.495			106.7	102.3	0.96
<i>Gribov (10MW U)</i>	.605	18	64.3		37.2	
<i>Gribov (10MW L)</i>	.605	20	53.2		60.2	
<i>Gribov (U+L)</i>	.605			91.2	97.4	1.07
<i>li=1.0 (10MW U)</i>	.730	18	62.75		32.2	
<i>li=1.0 (10MW L)</i>	.730	20	50.8		48.9	
<i>li=1.0 (U+L)</i>	.730			75.8	81.1	1.07

Table III

Case sob2	\square	\square_m	\square_m	J_{bs} (kA/m ²)	J_{peak} (kA/m ²)	J_{peak}/J_{bs}
<i>li=0.7 (10MW U)</i>	.735	18	58.2		39.4	
<i>li=0.7 (10MW L)</i>	.735	20	44.8		55.2	
<i>li=0.7 (U+L)</i>	.735			75.4	94.6	1.25
<i>Gribov (10MW U)</i>	.770	18	57.4		41.7	
<i>Gribov (10MW L)</i>	.770	20	44.5		55.6	
<i>Gribov (U+L)</i>	.770			72.3	97.3	1.35
<i>li=1.0 (10MW U)</i>	.825	18	57.7		38.1	
<i>li=1.0 (10MW L)</i>	.825	20	44.4		49.5	
<i>li=1.0 (U+L)</i>	.825			68.2	87.6	1.28

6. Effect of the local beam size on NTMs stabilisation efficiencies

It has been shown that a lower poloidal location of the launcher would optimize stabilization efficiencies [7,8]. Another possibility to increase the peak current density or equivalently to have a minimum profile width may be obtained by minimizing the local beam size. We consider here five beams characterized by the same waist $w_0 = 1.99$ cm (at e^{-2} of the power), with different distances (\square) of the waist from the mirror ($\square = -70$ cm, -20 cm, $+30$ cm, $+80$ cm, $+130$ cm, positive beyond the mirror, negative behind the mirror). The beams are launched from $R=656.4$ cm, $Z=413.5$ cm, with toroidal angle $\square=20^\circ$ and poloidal angles $\square=58.6^\circ$ and $\square=48.6^\circ$ to localise the driven current at $q=3/2$ and $q=2$ respectively. The distances of the two absorption zones from the mirror (Gribov case) are 175 cm for $q=3/2$ and 135 cm for $q=2$. Figs 5 and 6 show the current density profiles for 1 MW of EC power injected with different beams and the behaviour of both figures of merit as a function of the local beam size w respectively.

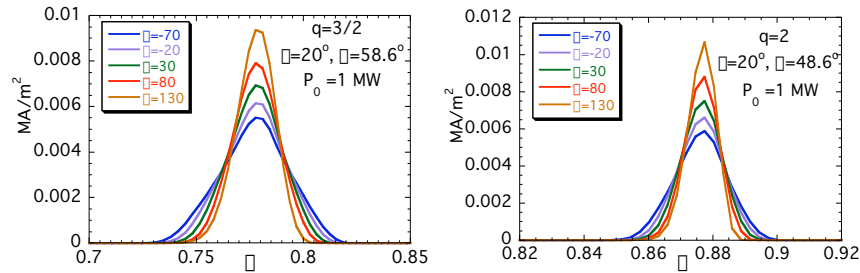


Fig.5: Current density profiles obtained with 1 MW EC power in different beams.

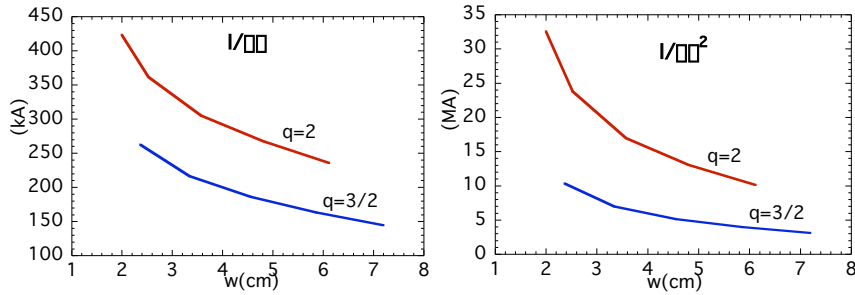


Fig.6: Figures of merit vs. local beam size

The above results have been obtained by varying the spot size w (in vacuum) over a quite wide range (up to a factor three). It is found that over the considered range and for these trajectories the profile width d scales linearly with the beam radius w (apart from w values close to the minimum beam radius $w_0=1.99$ cm), while the total current is almost constant.

Acknowledgement

This work is being carried out under the EFDA technology task TW3-TPHE-ECHULA.

References

- [1] H. Zohm et al., this Workshop
- [2] D. Farina, S. Nowak, G. Ramponi, IFP Report FP 03/6 (October 2003)
- [3] Y.Gribov, Plasma of ITER Scenario 2, 12/12/2002
- [4] A.Portone and G.Saibene, <http://efdasql.ipp.mpg.de/EUHandCD/ECRH/equilibria>
- [5] B.S.Q.Elzendorf et al., Conceptual design of the mm-wave layout for the RS Launcher, Sept.2003 <http://efdasql.ipp.mpg.de/EUHandCD/ECRH>
- [6] F.Volpe et al., this Workshop
- [7] B.Harvey, F.V.Perkins, Nucl. Fusion 41,1847 (2001)
- [8] G.Ramponi et al., Proc.of IAEA TM on ECRH Physics and Technology for ITER, Kloster Seon, July 2003